Ocean and Coastal Management 278 (2026) 108244

Contents lists available at ScienceDirect

Ocean and Coastal Management

journal homepage: www.elsevier.com/locate/ocecoaman

Sea level rise and storm surge impacts economic assessment on coastal infrastructure: Study case of the Llevant Main Sewer (Badalona, Spain)

Guillem Flor Tey [a], Joan Insa [a], Eduardo Martínez-Gomariz [a], Beniamino Russo [a,*], César Mösso [b], César Paradinas [c]

[a] Flumen Research Institute, Universitat Politècnica de Catalunya – BarcelonaTech (UPC), Campus Nord, C/Jordi Girona 1-3, Barcelona, 08034, Spain
[b] LIM – Maritime Engineering Laboratory Research Group, Universitat Politècnica de Catalunya - BarcelonaTech (UPC), Campus Nord, C/Jordi Girona 1-3, Barcelona, 08034, Spain
[c] FIC – Climate Resilience Foundation, C/Modesto Lafuente 45, Madrid, 28003, Spain

ARTICLE INFO

Keywords:
Coastal flooding
Risk assessment
Sea level rise
Adaptation measures
Wastewater infrastructure
Climate resilience
Barcelona metropolitan area

ABSTRACT

Coastal wastewater infrastructure is increasingly threatened by climate-induced hazards, yet quantitative risk assessments for such systems are still limited. This study evaluates the climate risk of the Llevant Main Sewer, a 10.8 km coastal-parallel sewer serving approximately 400,000 inhabitants in the eastern part of the Metropolitan Area of Barcelona (Spain), under four Shared Socioeconomic Pathway (SSP126, SSP245, SSP370, SSP585) scenarios up to 2100.

Hazard assessment was based on significant wave height and sea level rise projections derived from CMIP6 climate models, propagated to the sewer alignment using a linear coastal approach calibrated against the Barcelona buoy. Exposure and vulnerability were characterised through a Protection Level Index (PLI) that classifies sewer sections by their degree of coastal protection. Vulnerability functions relating repair cost per linear metre (€/ml) to storm surge intensity were developed from historical intervention records along the main sewer, providing novel empirical cost estimates that are scarcely documented for this type of infrastructure.

Integrating these three components, economic risk was estimated under Business-as-Usual scenario in which repairs are triggered only after storm-induced failure. A Cost-Benefit Analysis (CBA) comparing three adaptation strategies (damage repair, rock revetment enhancement, and layout relocation) was performed across all SSP scenarios. Results show that risk grows substantially under higher-emission pathways, with layout modification yielding the most favourable benefit-cost ratios for most scenarios. This framework provides a replicable methodology for assessing and managing climate risk in coastal sewerage systems, with direct impactions for infrastructure planning in other Mediterranean and coastal urban contexts.

1. Introduction

Currently, climate change is an unequivocal threat to our planet, and its most significant consequences are just beginning to unfold. As scientific evidence clearly demonstrates, this phenomenon leads to an increased frequency and intensity of extreme weather events and hazards, including flooding from intense rainfall and storms, droughts due to reduced precipitation, sea level rise (SLR), and higher temperature induced by global warming (IPCC, 2021).

Such events trigger a wide range of repercussions that directly impact the normal functioning of multiple human settlements, including cities, towns, and villages, with urban populations being particularly affected. In this context, climate change-related impacts can affect essential urban services, such as water and energy supply, which are crucial for the continuous functioning of cities for much of the world's population (Martínez-Gomariz et al., 2021; Russo et al., 2020).

In this regard, wastewater systems, including sewerage networks and treatment facilities, are key infrastructures for urban areas due to their essential roles in supporting human activities and ensuring sanitation safety. Nevertheless, climate change exposes this type of infrastructure at significant risk, particularly in coastal regions where hazardous events can occur simultaneously (Hughes et al., 2021). In these areas,

* Corresponding author.
E-mail addresses: guillem.flor@upc.edu (G. Flor Tey), joaninsaf@gmail.com (J. Insa), eduardo.martinez-gomariz@upc.edu (E. Martínez-Gomariz), beniamino.russo@upc.edu (B. Russo), cesar.mosso@upc.edu (C. Mösso), cesar@ficlima.org (C. Paradinas).

https://doi.org/10.1016/j.ocecoaman.2026.108244
Received 15 September 2025; Received in revised form 10 April 2026; Accepted 18 May 2026
Available online 22 May 2026

increased infiltration into the collection system poses an additional challenge when combined with sea level rise and rising groundwater levels (Cahoon and Hanke, 2017). At a global scale, sea level rise is not only increasing baseline water levels but also amplifying the impact of coastal hazards by altering wave dynamics and storm surge propagation along both natural and engineered shorelines.

Coastal flooding hazards such as sea level rise (SLR) and storm surge can produce severe damage to coastal infrastructure, and their frequency is expected to increase significantly in the future (Flood and Cahoon, 2011). These processes directly affect linear coastal infrastructure systems, whose functionality depends on both structural integrity and their interaction with surrounding coastal dynamics. A main sewer running parallel to the coastline, a common infrastructure in the environment of drainage systems, is particularly susceptible to these mentioned climate-related hazards (Hu et al., 2019). Impacts on coastal sewers usually trigger knock-on effects, primarily affecting the wastewater treatment plants as they are the destination of the conveyed wastewater (Friedrich and Kretzinger, 2012). Specifically, the most common direct damage is related to wave impact (i.e., exposed sewer) and damage caused due to coastal erosion. In this sense, direct damage to the outer part of the infrastructure can cause ruptures, fractures or clogging of the sewer (Hughes et al., 2021). This damage also generates beach and nearby aquatic areas pollution and clean-up costs (Martínez-Gomariz et al., 2021), and possible increases in internal transport fluxes due to the new inflow points generated (Friedrich and Kretzinger, 2012).

In view of this context, it is essential to develop rigorous methods for assessing the future risk of wastewater coastal structures in order to adopt adaptation measures that enhance their resilience to such upcoming events. While previous studies have focused on potential increases in flow due to infiltration and inflow from sewer ruptures (Sangsefidi et al., 2023; Spirandelli et al., 2018), the main objective of this risk assessment study on the sewer is to economically quantify the damage caused by wave action and storm surge on the infrastructure. The present research focuses on the Llevant Main Sewer, a sewer running parallel to the Badalona (Spain) coastline. In this project, risk assessment is understood based on the concept of the disaster risk triangle (Crichton, 1999), recently adopted by the IPCC (2023a), where risk is defined as the combination of hazard, exposure and vulnerability, using the following approach.

1.1. *Risk = vulnerability x hazard x exposure*

This research is conducted within the ICARIA Project framework (Leone et al., 2025), a European project funded by the European Commission under the Horizon Europe programme. The objective of the project is to promote the use of comprehensive asset-level modelling frameworks to achieve a better understanding of climate-related impacts (Russo et al., 2023). Within the project, this research has been conducted within the Barcelona Metropolitan Area (AMB) case study, in Spain. It builds upon the integration of oceanographic data, historical intervention records, and infrastructure characteristics to evaluate the economic risk posed by climate change to coastal main sewers.

Firstly, hazard is assessed using historical data and future projections of sea level and significant wave height (Hs) as key variables for Sea Level Rise (SLR) and storm surges, respectively. Projections are derived from the four Tier 1 Shared Socioeconomic Pathways (SSP) scenarios developed under the Coupled Model Intercomparison Project Phase 6 (CMIP6) (IPCC, 2021). The propagation towards the coastline is estimated using a linear-based approach. Secondly, exposure and vulnerability are assessed through the development of the Protection Level Index (PLI), which categorises sewer sections according to their level of protection (e.g., fully exposed, sand protection, rock revetment protection, or fully buried sewer).

Vulnerability assessment focuses on sewer segments with sufficient available data (in this case, for a fully exposed sewer and a sewer protected by rock revetment). The relationship between repair cost per linear meter (€/ml) and the hazard intensity is quantified. Two vulnerability functions have been developed: one for the unprotected sections and another for the sections protected by rock revetment. Finally, by integrating previous assessments, the study estimates the economic risk to the Llevant Main Sewer under four projected SSP scenarios up to the year 2100. The analysis is conducted under the "Business-as-Usual" (BAU) scenario, in which repairs to the sewer, or its protective rock revetment, are executed only after structural failure induced by storm events and wave action. Additionally, a Cost-Benefit Analysis (CBA) is included for all SSP scenarios, comparing the BAU strategy with two adaptation measures: (1) implementing or reinforcing the existing rock revetment and (2) fully modifying the sewer layout to relocate it to a non-exposed area.

2. Materials and methods

2.1. *Study area description*

The Metropolitan Area of Barcelona (AMB), an urban agglomeration that encompasses 36 municipalities spanning 636 km^2, is the largest conurbation in the western Mediterranean, housing over 3.2 million inhabitants (AMB, 2024a). The AMB, as the administrative entity overseeing the Metropolitan region, holds the ownership of the wastewater infrastructure, while Aigües de Barcelona is the mixed company responsible for managing wastewater conveyance and treatment processes from the household connections with the municipal sewer networks to the treatment plants (Martínez-Gomariz et al., 2021). The whole sanitation network of the Metropolitan Area is formed by five independent sanitation systems (AMB, 2024b). The Llevant Main Sewer is part of the Besòs sanitation system (Fig. 1), situated in the northern of the region. It extends from the municipality of Montgat to the Sant Adrià del Besòs wastewater treatment plant (WWTP).

The Llevant Main Sewer has a length of 10.8 km and serves 5 municipalities (Montgat, Tiana, Badalona, Sant Adrià del Besòs and Santa Coloma de Gramenet) (Martínez-Gomariz et al., 2021), providing wastewater services to approximately 400,000 inhabitants. Therefore, its existence is fundamental to ensuring sanitation safety in these served areas, because this coastal structure collects both wastewater and stormwater from the municipal sewer networks of the previously described Besòs sanitation system. Examining key structural characteristics, the Llevant Main Sewer is designed considering the contribution flow rates up to 2.4 times the average wastewater flow rate. Besides, it has an average slope of less than 0.1%. And 17 combined sewer overflow (CSO) structures, which activate when its capacity is exceeded. Additionally, 7 pumping stations are distributed along its alignment to facilitate flow conveyance (Meta Engineering, 2021).

Given the location of the studied infrastructure, the primary climate-related hazards posing direct damage include coastal flooding and compound flooding (a combination of coastal and pluvial), particularly during storm events. Fig. 2 shows the damage and structural failure affecting a section of the Llevant Main Sewer in Badalona, caused by a storm in 2020. As previously mentioned, this research puts the spotlight on Sea Level Rise (SLR) and Storm Surges (SS). Subsequently, both hazards are detailed and their impacts in the study area are accurately described.

2.2. *Coastal hazard concepts*

Sea level rise (SLR) refers to the increase in ocean levels, primarily driven by thermal expansion and the melting of land-based ice (NOAA, 2024). According to numerous studies, the Catalan coastline faces a worrying situation. The report published by the Catalan Government in 2021 called "Un litoral al límit" (Generalitat de Catalunya, 2021) revealed that the sea level in l'Estartit, a coastal municipality located 120 km northeast of Badalona, has risen by nearly 10 cm over the last 30

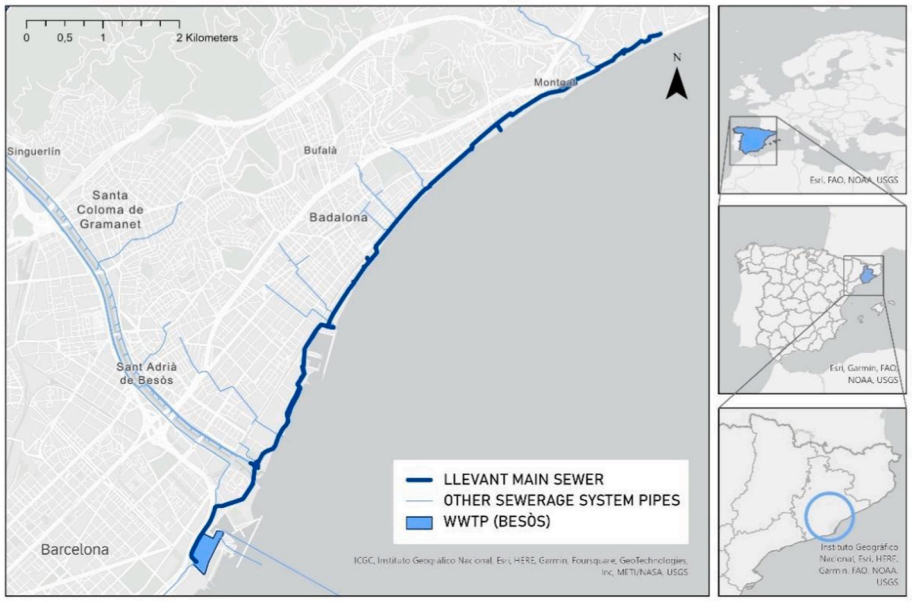

Fig. 1. Spatial location and layout of the Llevant Main Sewer in Badalona (Spain).

Fig. 2. Damage in a rock revetment section of the Llevant Main Sewer in Badalona, after a storm in 2020.

years, consistent with the observed Mediterranean wide trend of approximately 4 mm per year. Besides, only 20% of the Catalan coast has enough accommodation space to continue retreating in response to rising sea levels. Since 2017, a significant regression of beaches has been observed along certain sectors of the metropolitan coast, with average retreat rates reaching 9.8 m/year in Badalona and 7.5 m/year in Montgat. In view of this context, this project analyses various SLR projections of the study area to assess their potential impact on the Llevant Main Sewer.

Storm surges are a climate-related hazard characterised by an abnormal rise in sea level along coastal areas during extreme weather events. This phenomenon is produced because of wind forces and atmospheric pressure changes. Moreover, SLR plays a critical role in amplifying storm surges by rising baseline sea levels, thereby enhancing inundation extent and contributing to higher peak surge heights during extreme weather events (Tebaldi et al., 2012).

It must be highlighted that wave action is a dynamic process intricately linked to storm surges. In this sense, the widespread rise in sea level leads to increased water depth, which in turn results in higher wave heights. According to the report published by the Catalan Government (SMC, 2021), between 1990 and 2020, a total of 164 rough weather events with significant wave heights (Hs) ranging from 4 to 9 m

were recorded along the Catalan coast, averaging five events per year. Notably, the report concluded that 40 % of these events were classified as cyclone-type storms, which are responsible for generating storm surges. Herein, the present study analyses various significant wave height projections to assess their potential impact on the Llevant Main Sewer.

In the ICARIA project, the concept of Extreme Sea Level (ESL) is understood as the combined effect of wave action, tides, and sea level rise. In the present study, however, we do not use the ESL in its standard hydrodynamic sense. Instead, this concept has been replaced by the Extreme Event Sea Level (EESL), as a conservative hazard proxy obtained by combining the significant breaking wave height at the coastline with the projected sea level rise. EESL is not interpreted as a physically exact still water level, since wave height is not directly additive to sea level in strict hydrodynamic terms. Rather, it is used here as an impact-oriented screening indicator to approximate the combined effect of background water-level increase and wave-induced coastal loading on the exposed sewer sections. Astronomical tides were not explicitly included in this indicator because the study area is microtidal and, in a long-term scenario-based analysis, the coincidence between future extreme events and a specific tidal phase cannot be prescribed deterministically. Therefore, for the purpose of asset-level comparative risk assessment, tides were considered to have a second-order influence relative to the wave-breaking component and projected sea level rise.

2.3. Hazard assessment

The hazard assessment was conducted using a robust yet simplified approach, based on realistic climate projections. One of the outcomes of the ICARIA project was the projection of several climatic variables and the statistical downscaling across the entire AMB, including wave height and sea level. These climate projections have been published in an open access data repository (Paradinas et al., 2024). For this research, average daily significant wave height (Hs) data from January 1, 2021, to December 31, 2100 were used, based on the known as Tier 1 climate scenarios, SSP126, SSP245, SSP370 and SSP585, with eight CMIP6 climate models per scenario. Additionally, SLR data has been provided for the same period, using the same four climate scenarios. This study has used historical records form a buoy belonging to the *Puertos del Estado* network, as in other similar researches conducted in Spain (Megías and García-Román, 2024). Specifically, the measurement point for this case of study is the Barcelona Buoy II, a monitored buoy located off the Port of Barcelona.

The four climate scenarios project different climatic conditions based on emission level, economic development, and sustainability trends. Thus, SSP126 and SSP585 represent the most optimistic and the most pessimistic scenarios, respectively, while SSP245 and SSP370 correspond to intermediate pathways (IPCC et al., 2023b). For variables like temperature and SLR, which have a direct and well-understood relationship with greenhouse gas concentrations, SSP scenarios provide a clear framework for projections. However, for variables like significant wave height (Hs), which are influenced by a complex interplay of factors, the relationship with SSP scenarios is less direct. Therefore, while SSP scenarios can be used to project changes in wave height, the projections may not follow the same pattern observed with temperature or SLR increases.

2.3.1. Storm surges data processing

This step of the research has consisted of extracting the storm events registered by each climate-scenario by means of a python code. Concretely, each scenario has its own folder with the 8 mathematical models' outputs in. txt files. Hence, the code has been run four times (one per folder). The significant wave height (Hs) data are recorded daily. The definition of a storm event along the Catalan coast is established in the Recommendations for Maritime Works (ROM, 1992), which specifies that a storm event occurs whenever the significant wave height (Hs) exceeds 2 m for more than 24 h. Accordingly, we deem a storm valid when two consecutive data points surpass the 2 m threshold. Storm duration is then calculated as the number of such consecutive values multiplied by 24 h. Apart from the storm number and duration, this data treatment has allowed us to identify the following attributes for each of the four climate-scenarios.

- **Model:** BCC-CSM2-MR, CanESM5, CMCC-ESM2, CNRM-ESM2-1, EC-EARTH3, MPI-ESM1-2-HR, NorESM2-MM and UKESM1-0-LL.
- **Event number:** List of events per model (storm 1, storm 2 …).
- **Event data:** Hs values $\geq$ 2 m contained in each storm.
- **Hsmax (m):** Highest value registered in each storm data interval.
- **Event duration (h):** Value multiple of 24 corresponding to the duration of each event.
- **Event date:** Storm start dates (Jan 1, 2021 - Dec 31, 2100).

The same temporal horizons used are 2021–2040, 2041–2070, and 2071–2100, aligning with the ICARIA project framework. For each scenario and period, the 0^{th}, 30th, 50th, and 90th percentiles of the maximum Hs variable (Hsmax) have been obtained, considering the variability of the models used. The percentiles 50th and 90th are commonly used in the literature to represent typical and high-energy coastal wave conditions (Laino and Iglesias, 2024).

In the present study, the 30th percentile is also included to characterise frequent, moderate wave conditions. Although not associated with extreme events, these conditions may exert continuous pressure on the operability, maintenance, and accessibility of coastal infrastructure. While the application of lower percentiles such as 30th is uncommon in wave climate studies, this approach is consistent with practices in other domains of climate and hydrological analysis, such as urban planning, thermal comfort assessment, or evaluations of moderate precipitation, and supports a more granular and operationally relevant representation of climate impacts under future scenarios. Moreover, the median value of the significant wave height recorded at the Barcelona buoy during storm events observed since 2016 is slightly above 2.50 m, which is consistent with the 30th percentile values across the different future climate scenarios. Additionally, the 0^{th} percentile is included, based on the criterion that all wave events exceeding 2 m are considered potentially damaging, thereby establishing a lower threshold for impact relevance. Moreover, the number of events associated with each percentile has been determined. In parallel, the temporal variation of this variable over the entire period has been examined. Thanks to this distribution, it could be observed that, for each of the climate scenarios, the temporal variation of the variable is negligible, with a slight increase in number of events under the SSP585 scenario, particularly for lower return period events.

Fig. 3 illustrates the values of the previously mentioned percentiles for the SSP126 scenario. Besides, Fig. 4 presents the temporal distribution of Hsmax under the same scenario. Equivalent plots have been generated for the remaining climate-scenarios and have served as the basis for Table 1, which compile the percentile values by scenario and period, as well as the corresponding number of associated storm events, respectively.

2.3.2. Wave propagation

As the oceanographic data were obtained from the Barcelona Buoy II, located off the coast at a depth of approximately 68 m, it is necessary to propagate these data to coastal locations near the Llevant Main Sewer. To achieve a propagation predominantly perpendicular to the sewer's coastline, the data from Barcelona Buoy II were transferred to SIMAR point 2112137 (Fig. 5).

This extrapolation is considered valid, as both locations share similar depths and share the same coastal orientation. To carry out the propagation, the peak period (Tp) and direction (θ) have been estimated based on section E of the ROM atlas. The former (Tp) has implied the representation of a historical series of Hs (axis x) and Tp (axis y) between

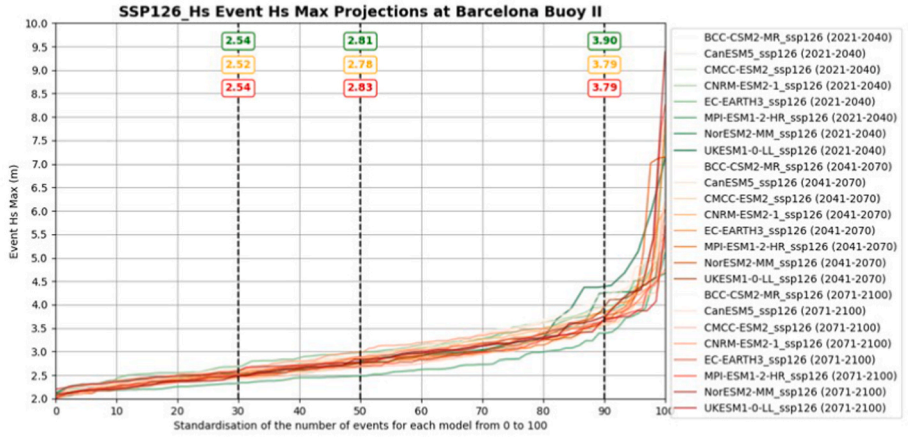

Fig. 3. Identification of the 30th, 50th, and 90th percentile thresholds across the SSP126 scenario dataset. Green 2021-2040, Yellow 2041-2070, Red 2071-2100. (For interpretation of the references to colour in this figure legend, the reader is referred to the Web version of this article.)

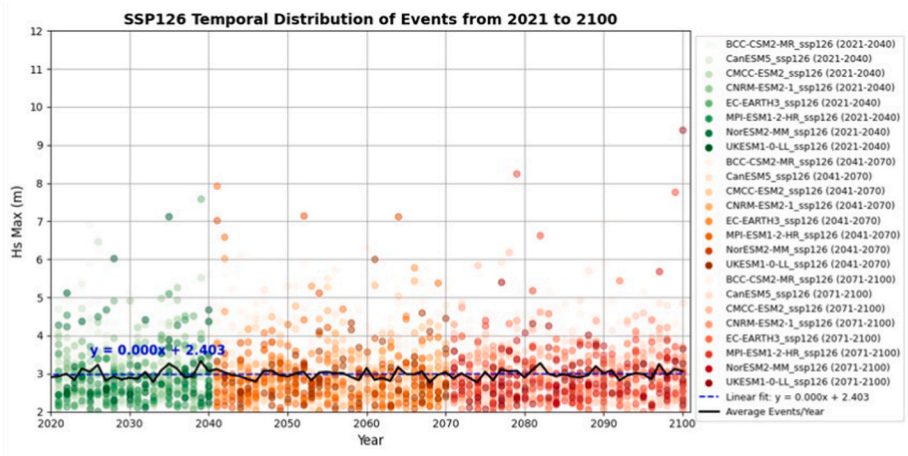

Fig. 4. Temporal distribution of events from 2021 to 2100 under SSP126 scenario. Green 2021-2040, Yellow 2041-2070, Red 2071-2100. (For interpretation of the references to colour in this figure legend, the reader is referred to the Web version of this article.)

Table 1
Max Hs and Number of Events for 0th, 30th, 50th and 90th percentiles per period and climate scenario.

Climate-scenario	Time period	Max Hs results (m) (left) and Number of events (right)								Total N° Events
		0th percentile[a]		30th percentile		50th percentile		90th percentile		
SSP126	2021-2040	2.00	31	2.54	20	2.81	40	3.90	10	100
	2041-2070	2.00	44	2.52	31	2.78	57	3.79	15	147
	2071-2100	2.00	44	2.54	29	2.83	57	3.79	15	145
SSP245	2021-2040	2.00	30	2.53	20	2.08	38	3.86	10	98
	2041-2070	2.00	42	2.58	28	2.85	54	3.96	14	138
	2071-2100	2.00	42	2.5	28	2.79	55	3.78	14	139
SSP370	2021-2040	2.00	32	2.52	21	2.78	42	3.75	11	106
	2041-2070	2.00	44	2.51	29	2.73	57	3.79	15	145
	2071-2100	2.00	42	2.50	26	2.75	54	3.75	14	136
SSP585	2021-2040	2.00	36	2.53	24	2.81	46	3.8	12	118
	2041-2070	2.00	50	2.54	33	2.81	64	3.75	17	163
	2071-2100	2.00	45	2.51	29	2.79	57	3.82	15	146

[a] The 0th percentile is included, as all identified events exceeding 2 m have been considered damaging. The number of events in those cells corresponds to the events falling between 0th and 30th percentiles.

2015 and 2024 provided by Puertos del Estado (2004).

Consequently, Equation (1) has been used, enabling the calculation of Tp from Hs values:

$$Tp = 6.243 \times Hs^{0.5} \quad (1)$$

The latter (θ) has been determined using the wind rose associated with SIMAR point 2112137. Analysis of this data reveals that the predominant wave directions are East (E), East-Southeast (ESE) and South (S). Given that this research focuses on assessing future impacts, the study has opted to consider the most harmful direction. To determine it, the wave approach angle (α) of each section has been calculated for the three directions following the subsequent steps.

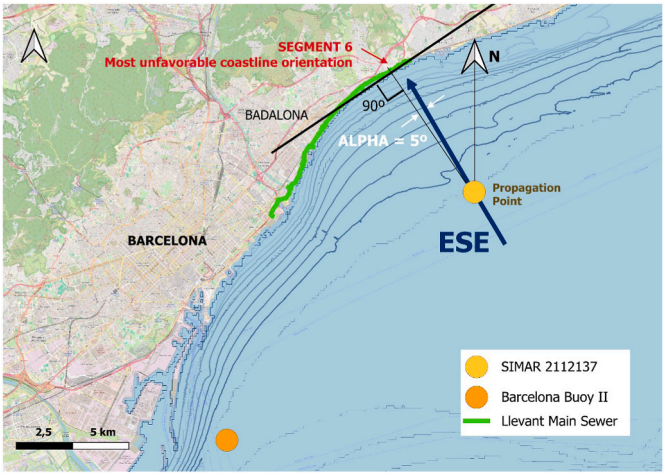

Fig. 5. Bathymetry of the study area. Selected propagation point and design direction.

1. Calculation of the angle between the considered section and North.
2. Sum of the previous angle plus 90° (projection).
3. Calculation of the absolute difference between the previous sum and the θ considered.

As ESE provides the lowest values of α, it has been considered the design direction. Among all the sections, the most critical value of (α) is 5°. In order to remain on the side of safety, the wave propagation is carried out using this angle. Consequently, for each wave height value (percentile), a single propagated wave height value - common to all sections - is obtained. Hereunder, Fig. 5 shows both the propagation point and design direction.

Subsequently, next step is to define a wave propagation model. Considering that this study relies on projections, which inherently involve uncertainty, a Python-based linear propagation model is deemed appropriate. This model, is primarily based on the simplification of shoaling (Ks) and refraction (Kr) coefficients, derived from the principle of energy conservation between two arbitrary consecutive deep-water sections (UPC, 2014).

Nonetheless, since this investigation requires wave propagation towards the coast (shallow water), the concept of wave breaking must be considered (Bergillos, 2016). In this regard, the model integrates wave breaking effects using Yashimi Goda's empirical expression, commonly referred to as Goda's gamma (γ_b). Overall, the linear propagation model applied in this research follows the subsequent governing Equations (2)–(5):

$$H_b = \gamma_b \cdot h_b \tag{2}$$

$$H_b = 0.17 \cdot L_0 \left[1 - exp\left(-1.5(\pi \cdot L_0\, h_b)(1 + 11 \cdot tan(\beta))^{\frac{4}{3}}\right)\right] \tag{3}$$

$$H_b = H_1 \cdot \sqrt{\frac{C_{g1}}{C_{g2,b}}} \cdot \sqrt{\frac{cos(\alpha_1)}{cos(\alpha_{2,b})}} \tag{4}$$

$$\alpha_{2,b} = arcsin\left[sin\left(\alpha_1 \cdot L_2 \,/\, L_1\right)\right] \tag{5}$$

Where H_b is the wave breaking height (output of the model) and is optimised by γ_b.

2.3.3. SLR data processing

Regarding SLR, only basic graphical processing has been applied, as the dataset was smaller and did not require additional calculations. Thus, Fig. 6 presents a comparison between the four climate scenarios throughout the time series. In this case, the expected theoretical behaviour of the scenarios is observed, with SSP585 predicting the highest SLR of 88 cm by the year 2100.

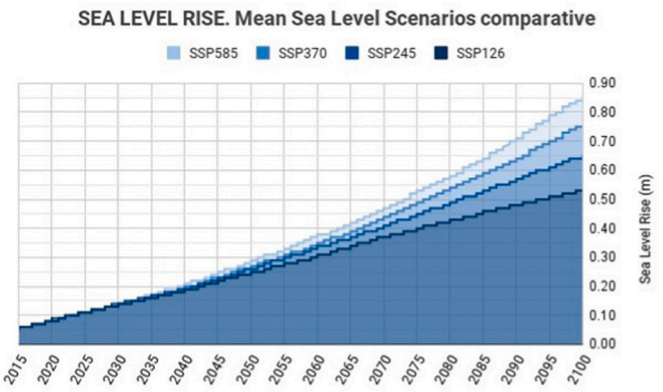

Fig. 6. Sea level rise on the AMB coast. Results of the downscaling performed in the ICARIA project.

Finally, the water level at the coastline used in the hazard assessment is determined by integrating both climate-related hazards through a simplified hydrostatic approach based on a bathtub model. Bathtub models (BTH) are coastal flood models typically employed at global or regional scales due to their computational efficiency (Kasmalkar et al., 2024). Also known as static or equilibrium flood models, they estimate flood depths by calculating the difference between the projected water level and the ground elevation. Although the BTH is commonly used for permanent flooding, in this study the same methodology has been applied to identify areas potentially exposed due to the already defined Extreme Event Sea Level (EESL). In this way, the mean SLR contributions from the three time periods (2021-2040, 2041-2070, 2071-2100) have been added to the Hb results from the propagation.

It should be noted that linear wave propagation in shallow coastal environments has well-known limitations. In particular, the adopted scheme does not explicitly resolve bottom-friction dissipation, nonlinear wave transformation in the surf zone, diffraction/reflection induced by coastal structures, wave setup, or storm surge–wave interactions. Therefore, the resulting breaking wave height (Hb) and the derived bathtub height (BTH, here EESL) should be interpreted as simplified proxies of coastal loading rather than as full reconstructions of extreme event sea levels. Nevertheless, for the purposes of this study, namely, asset-level climate risk screening and comparison of adaptation strategies, the approach provides a practical first-order estimate of wave-induced forcing while preserving transparency and applicability for infrastructure managers.

2.4. Exposure and vulnerability assessment

As previously introduced, the Protection Level Index (PLI) has been developed based on a visual classification of the sewer protection and field inspections at selected locations. Specifically, this index distinguishes different sections of the Llevant Main Sewer according to their degree of protection, categorised into five levels presented in Table 2.

Hence, this classification is applied to the layout of the Llevant Main Sewer. The results are shown in Fig. 7, where 10 different sections have been obtained. As illustrated in the image above, three sections have been assigned a PLI of 1: Patins de Vela beach, the northern CSO, and the sewer branch of Mar School. Additionally, the section known as 'Les Tres Xemeneies' has been classified with a PLI of 2, while the Barca Maria Beach section has been classified with a PLI of 3. The remaining sections are protected and have been assigned a PLI of 4.

To determine which of the areas considered exposed ($0 > PL > 3$) are reached by the water column (EESL), a spatial analysis was conducted using the QGIS tool. For this purpose, 2x2 raster maps of the study area

Table 2
Definition of the characteristics of the different Protection Level (Protection Level Index).

PROTECTION LEVEL 0. Unprotected areas, garnet red.
The main sewer is visible to the naked eye from the waves. Exposed.
PROTECTION LEVEL 1. Sand protection, red.
The main sewer remains buried or semi-buried in sand against the waves and is exposed with the first coastal sand erosion. Exposed.
PROTECTION LEVEL 2. Rock revetment protection, orange.
The main sewer remains protected by a rock revetment embankment that reduces the impact, if any, of wave intensity on the main sewer. Exposed.
PROTECTION LEVEL 3. Rock revetment and sand protection, yellow.
Sum of the two previous protections. Exposed.
PROTECTION LEVEL 4. Protection by urban infrastructure, green.
The main sewer is buried and protected by structural elements such as buildings or the promenade in the area. Non-exposed.

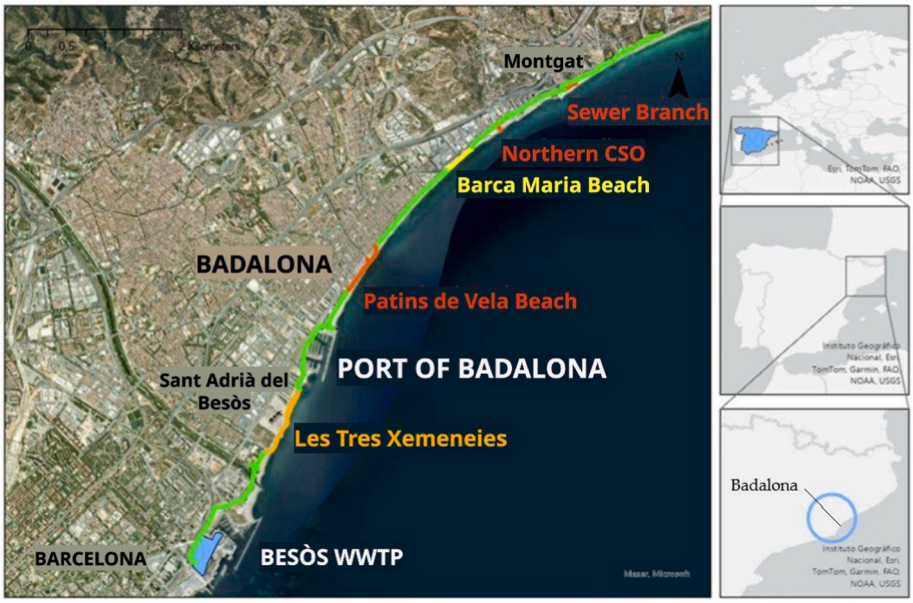

Fig. 7. Application of the PLI to the Llevant main sewer.

(ground elevation) were used (ICGC, 2024). Based on the difference between the EESL values and these ground elevations (i.e., flood depth), and by overlaying the resulting values with the exposed areas, the number of linear meters affected (both in unprotected zones and in areas protected by rock revetment) were obtained for each EESL considered.

Additionally, the analysis allowed for the identification of both the most favourable and the most critical coastal flooding situations (Figs. 8 and 9). While the most favourable situation results in minimal impact, under the most unfavourable scenario all sections classified as exposed are completely flooded.

The vulnerability assessment is constrained by the availability of historical intervention data for the sewer. As this information is difficult to obtain, since it is held by private entities and the relationship between a storm event and the repair cost is not direct, the scientific value and contribution of the proposed methodology lie in providing initial reference values that can serve as an order of magnitude of the damage quantification. A total of 13 interventions affecting the sewer or its protective structures were identified between 2015 and 2022. To facilitate data processing, protection groups PLI 0 and PLI 1 have been combined into one category, while PLI 2 and PLI 3 have been grouped together. It has been ensured that storm events impacting areas classified as PLI 1 or PLI 3 (where meters of sand are present in front of the sewer) have resulted in the removal of protective sand, leading to direct exposure of the sewer or the rock revetment protection to wave impact. PLI 4 has not been evaluated, as its exposure is considered negligible, and consequently, the associated cost is assumed to be zero.

The vulnerability definition process aims to determine the repair cost (€ per linear meter) associated with specific oceanographic or hazard conditions, following a methodology similar to that used in studies of other infrastructure assets, where the hazard driver is the flood water level (Martínez-Gomariz et al., 2020). The development of the vulnerability assessment has been carried out following the workflow outlined below.

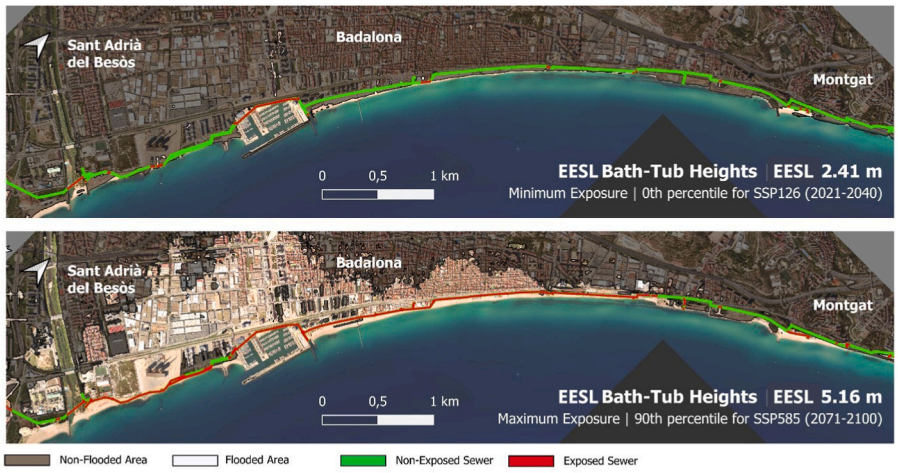

Fig. 8. Most favourable and critical situations of projected coastal flooding events (EESL water height) for 2015-2100 for all the Llevant Main Sewer extension.

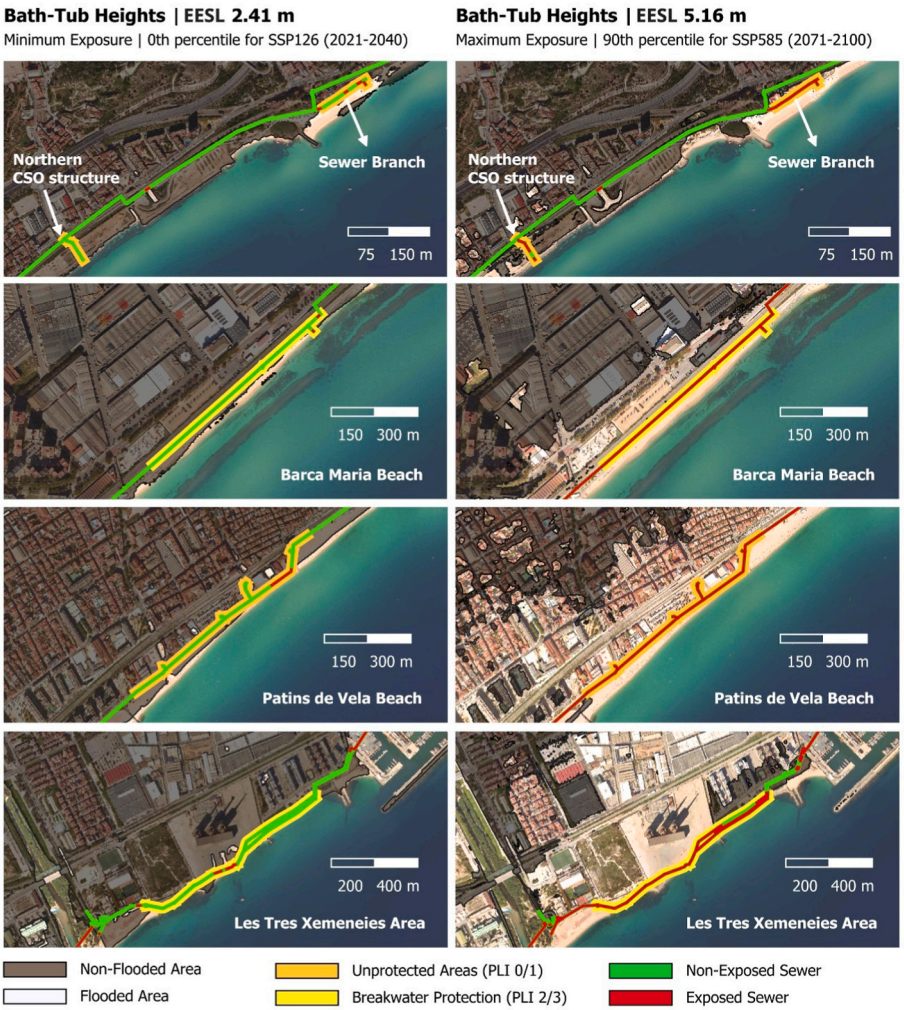

Fig. 9. Most favourable and critical situations of projected coastal flooding events (EESL water height) for 2015-2100 for unprotected areas (PLI 0/1) and rock revetment protection (PL 2/3) of the Llevant Main Sewer. The sections shown correspond to those identified as potentially exposed and presented in Fig. 7.

1. Identification of historical repairs conducted by Aigües de Barcelona on the sewer or its rock revetment protection, including affected area and associated PLI, date of reparation, intervention cost, and affected linear meters.
2. Identification of historical storms events within the intervention time frame. A storm event is assumed when hourly records at Barcelona Buoy II exceed 2 m for at least 24 consecutive hours (ROM, 1992).

3. Propagation of the storm's average significant wave height (Hs) to the coast, following the same procedure described in Section 2.2 for future projection data.
4. Correlation of historical repairs with past storm events. The total repair cost is distributed across the number of storms occurring since the previous intervention, proportionally divided based on each event's duration.
5. Standardisation of the storm event Hs (Hs EVENT) relative to the maximum recorded Hs at Barcelona Buoy II (5.48 m on 7 February 2023). The hazard driver (ϕ) is defined as ϕ = Hs EVENT/Hs MAX.
6. Establishment of the relationship between ϕ and repair cost per meter (ϕ vs €/ml) for the different exposure levels (PLI) previously assigned.
7. Identification of trends and construction of vulnerability graphs for the fully exposed sewer (Fig. 10a) and the sewer protected by rock revetment (Fig. 10b).

As shown in Fig. 10a, which corresponds to unprotected sections, three zones have been identified: no damage for $\phi < 0.4$, a repair cost of 250 €/ml for $0.4 < \phi < 0.57$, and the highest repair costs (1800 €/ml) for $\phi > 0.57$. Conversely, Fig. 10b, which represents sections with rock revetment protection, indicates that historical data do not establish a clear relationship between ϕ and specific costs. Therefore, a fixed repair cost of 500 €/ml is assigned for all events, as it represents a reasonable average value.

2.5. Risk assessment and adaptation measures – cost benefit analysis (CBA)

In this research, the economic risk is defined as the potential financial losses resulting from the impact of the studied climate-related hazards (SLR and storm surges) on the Llevant Main Sewer. Subsequently, two adaptation measures are analysed and compared with the BAU scenario using a cost-benefit analysis (CBA) for each SSP scenario. Given the significant exposure of certain sections of the study infrastructure, the following alternatives have been considered.

a. BAU scenario: main sewer repair upon damage. This approach involves repairing the main sewer whenever damage occurs for unprotected sections in which protected measures have not been projected. For $\phi < 0.57$, the associated cost 250 €/ml, while for $\phi > 0.57$, the cost increases to 1800 €/ml, based on the sewer vulnerability assessment. Costs have been estimated using a linear cost approximation calculated by dividing the total repair cost of the different sections by the corresponding length of the intervention.

Two protection measures have been assessed. The linear cost associated with their implementation has been derived from an Alternatives Study of specific sections of the Llevant Main Sewer, conducted by Meta Engineering SA (2021) as part of a preliminary study requested by the Metropolitan Area of Barcelona.

b. Adaptation Measure 1: Implementation and maintenance of rock revetment protection. This approach involves employing one of the most typical hard engineering measures to protect coastal structures. The initial implementation unit cost is approximately 3700 €/ml (Meta Engineering, 2021), with an additional 500€/ml required for maintenance and replacement following each damaging event. As a result, the initial cost of implementing rock revetment protection (without the replacement component) can be calculated with Equation (6):

$$Rock\ revetment\ implementation = 3700\ €/lm \times L_{Unprotected\ sections} \quad (6)$$

c. Adaptation Measure 2: Main sewer layout modification. This measure consists of raising the studied infrastructure to higher elevation to reduce exposure to coastal hazards. The estimated implementation cost is 11600 €/ml (Meta Engineering, 2021), with a projected service life of 70 years (Kaempfer and Berndt, 1999). This value includes both the construction cost of the sewer, and the cost of temporally bypass works during the construction period to mitigate risks associated with this phase. Thus, at the end of the considered time period (2021-2100), the total costs of modifying the sewer layout for unprotected sections and for sections protected by rock revetment can be calculated with Equation (7) and Equation (8) respectively:

$$Layout\ modification = 2 \times \left(11600\ € \,/\, lm \times L_{Unprotected\ sections}\right) \quad (7)$$

$$Layout\ modification = 2 \times \left(11600\ € \,/\, lm \times L_{R\ revetment-protected\ sections}\right) \quad (8)$$

The costs of rock revetment implementation and the sewer relocation remain constant across all climate scenarios, as they are independent of the storm events. In contrast, costs under BAU scenario and the reactive repair component of Adaptation Measure 1 (AM 1) vary with the intensity and frequency of projected hazards. Equation (9) presented below is proposed to evaluate the economic risk associated with each climate scenario. This expression integrates the results from the hazard assessment (percentiles and number of events), the exposure assessment (affected linear meters), and vulnerability assessment (cost per linear meter). The equation is applied separately to unprotected sections and those protected by rock revetment. Furthermore, it is adapted depending on whether BAU scenario or replacement component of AM 1 is considered. Hence, the cost for a given period and climate scenario has been computed as it follows:

$$Cost = \sum_{i=1}^{4} \left(Number\ of\ events \times Affected\ lm \times \frac{€}{lm}\right) \quad (9)$$

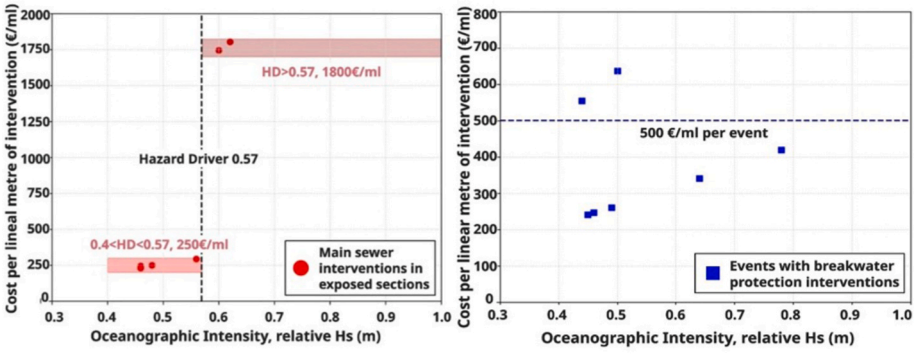

Fig. 10. Vulnerability Assessment associated with unprotected sections (PLI 0 and 1) on the left (a) and associated with rock revetment-protected sections (PLI 2 and 3) on the right (b).

In the equation presented above, each term of the summation corresponds to one of the four percentiles considered (0th, 30th, 50th and 90th). Within each term, the number of events associated with the given percentile is combined with the linear meters affected (according to the corresponding EESL) and the unit cost associated with the respective hazard driver (ϕ). By calculating the costs in the same manner for the remaining two periods and summing the results, the cumulative costs of the BAU approach and AM 1 over the entire 2021–2100 period are obtained. The same methodology is applied to all climate scenarios. Given the limitations and uncertainties inherent in both the vulnerability assessment and future climate projections, future costs have not been adjusted to projected price levels. This is because the focus of the study lies in the relative comparison between the different alternatives and the BAU scenario; therefore, the comparative results remain robust even without updating future cost values. Finally, to enhance clarity regarding the applied risk assessment methodology, a flow diagram has been developed and is presented in Fig. 11.

3. Results

3.1. Hazard and exposure assessment results

By applying the linear propagation model proposed in Section 2.2 to the maximum Hs percentiles presented in Table 1, the corresponding Hb values in the coastline area are obtained, as shown below in Table 3. Additionally, based on the sea level rise (SLR) data processing, mean SLR values have been calculated for each temporal period and climate scenario. As previously explained, by summing the Hb values with the corresponding mean SLR, Table 4 is obtained, which displays the EESL (representing the height of the water column). Finally, by dividing the EESL values by the maximum wave height recorded in the area (5.48 m), the respective ϕ values are determined (which are used to estimate the cost per meter associated with each event).

Similar to the maximum Hs data, there is no clear trend over time or across climate scenarios in the magnitude of the Hb variable. In contrast, with regard to the total number of events, a clear increase is identified in SSP585 scenario (see Table 1). Moreover, a clear upward trend is observed in the SLR variable, both over time and among different climate scenarios. The behaviour of this latter variable is consistent with expectations, as it is directly related to the level of emissions, which constitutes the main underlying factor of such scenarios.

According to results in Table 4, the EESL values range between 2.41 m and 5.16 m. Therefore, clear differences will exist in terms of coastal flooding levels (affected linear meters), which must be accurately assessed. To this end, a spatial analysis has been conducted using QGIS, enabling the association of each EESL value with a corresponding affected sewer length. Besides, it is important to highlight that most of ϕ values—except for those associated with 0th and 30th percentile in the first period—are greater than 0.57. This implies that a considerable proportion of the events will result in an impact of €1800 per linear meter in unprotected sections.

By means of such spatial analysis, the exposure assessment results in Table 5 present the linear meters affected in both unprotected sections and sections already protected by rock revetment, according to each climate-scenario and time period. Additionally, Figs. 12 and 13 which show the affectation of such types of sections have been built up. Both graphs group the data according to each type of percentile (0th, 30th, 50th and 90th) so as to illustrate in a better way how the impacted linear meters vary according to each time period and climate-scenario.

In all cases, the affected linear meters clearly worsen over time. That is, for a given percentile, the length of impacted sewer increases as we move forward through the time periods. Additionally, for both

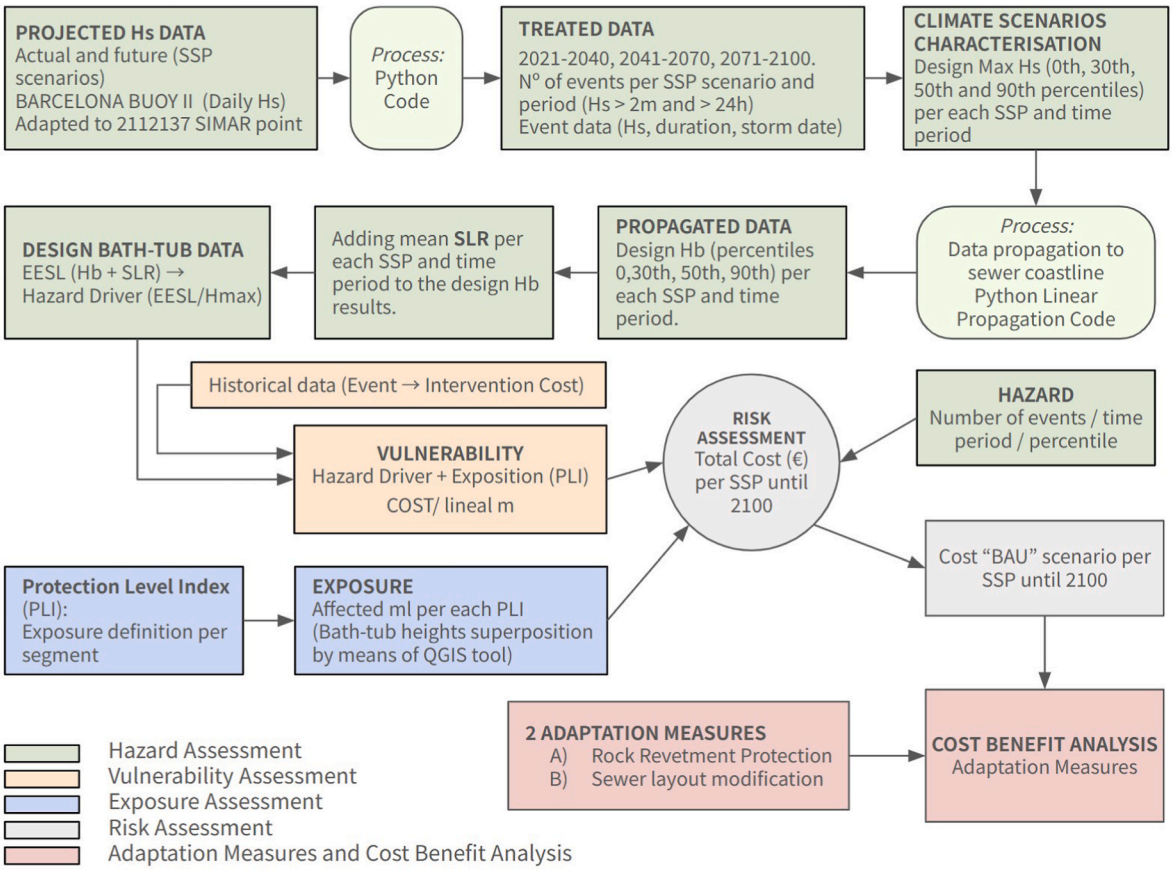

Fig. 11. Risk assessment methodology workflow resume for the Llevant Main Sewer.

Table 3
Results of the linear propagation (from Hs to Hb) and SLR per period and climate scenario.

Climate-scenario	Time period	Mean Sea Level (m)	Hb results (m)			
			0^{th} percentile	30th percentile	50th percentile	90th percentile
SSP126	2021-2040	0.14	2.27	2.92	3.25	4.64
	2041-2070	0.28	2.27	2.90	3.22	4.50
	2071-2100	0.45	2.27	2.92	3.28	4.50
SSP245	2021-2040	0.14	2.27	2.91	3.24	4.59
	2041-2070	0.30	2.27	2.97	3.30	4.71
	2071-2100	0.53	2.27	2.88	3.23	4.48
SSP370	2021-2040	0.14	2.27	2.90	3.22	4.44
	2041-2070	0.31	2.27	2.88	3.16	4.50
	2071-2100	0.59	2.27	2.88	3.18	4.44
SSP585	2021-2040	0.14	2.27	2.91	3.25	4.51
	2041-2070	0.33	2.27	2.92	3.25	4.44
	2071-2100	0.65	2.27	2.88	3.23	4.53

Table 4
Extreme Event Sea Level (EESL) as the sum of Hb and SLR, and Hazard driver results, as the division between EESL and 5.48 m (the maximum Hs registered in the Barcelona Buoy II).

Climate-scenario	Time period	EESL results (m) (Hb + SLR) and ϕ results (EESL/5.48 m)							
		0^{th} percentile		30th percentile		50th percentile		90th percentile	
SSP126	2021-2040	2.41	0.44	3.06	0.56	3.39	0.62	4.78	0.87
	2041-2070	2.55	0.46	3.18	0.58	3.5	0.64	4.78	0.87
	2071-2100	2.72	0.5	3.38	0.62	3.73	0.68	4.95	0.9
SSP245	2021-2040	2.41	0.44	3.05	0.56	3.38	0.62	4.73	0.86
	2041-2070	2.57	0.47	3.27	0.6	3.6	0.66	5.01	0.91
	2071-2100	2.8	0.51	3.41	0.62	3.76	0.69	5.02	0.92
SSP370	2021-2040	2.41	0.44	3.03	0.55	3.36	0.61	4.58	0.84
	2041-2070	2.58	0.47	3.2	0.58	3.47	0.63	4.81	0.88
	2071-2100	2.86	0.51	3.47	0.63	3.77	0.69	5.03	0.92
SSP585	2021-2040	2.41	0.44	3.05	0.56	3.4	0.62	4.65	0.85
	2041-2070	2.6	0.48	3.26	0.59	3.59	0.65	4.78	0.87
	2071-2100	2.92	0.53	3.54	0.65	3.88	0.71	5.16	0.95

Table 5
Affected linear meters for unprotected sections (left) and rock revetment-protected sections (right) per scenario, time period and percentile.

Climate-scenario	Time period	Affected linear meters (m) for unprotected (left) and rock revetment-protected (right) sections							
		0^{th} percentile		30th percentile		50th percentile		90th percentile	
SSP126	2021-2040	93	69	311	132	495	336	873	1322
	2041-2070	162	80	346	168	575	442	873	1322
	2070-2100	236	93	495	336	800	863	882	1508
SSP245	2021-2040	93	69	308	129	495	336	873	1267
	2041-2070	171	80	412	227	663	511	889	1573
	2070-2100	255	101	520	356	808	893	889	1581
SSP370	2021-2040	93	69	303	129	489	330	873	1141
	2041-2070	171	80	355	183	561	419	876	1328
	2070-2100	267	112	561	419	808	902	895	1585
SSP585	2021-2040	93	69	308	129	500	342	873	1166
	2041-2070	175	82	391	206	659	505	873	1322
	2070-2100	282	120	633	472	813	939	910	1644

unprotected sections and those protected by rock revetment, a clear upward trend is observed during the 2071–2100 period across climate scenarios. This occurs because SLR has a more pronounced influence in that period.

Finally, it is important to note that unprotected sections show significant impacts even at lower percentiles (with considerable values already appearing at 30th percentile). In contrast, this is not the case for sections protected by rock revetment; higher levels of impact begin to be noticeable at higher percentiles.

3.2. Risk assessment and adaptation measures – CBA results

This section details the costs associated with the BAU scenario and each adaptation measure (AM) across the four climate scenarios (Tables 6 and 7). Additionally, the economic comparison between them is presented in terms of money saved, expressed as the percentage gained when implementing one measure over another. Finally, the year at which one alternative becomes more economically viable than another is indicated.

The cumulative cost estimations presented area approximately four time higher than current figures reported by Aigües de Barcelona, suggesting a likely overestimation. Despite these limitations, addressed in detain in the Discussion section, the data still provide valuable insights. Notably, for both unprotected and rock revetment-protected sections, climate scenarios SSP126, SSP245, and SSP370 show no substantial cost differences between them. Conversely, scenario SSP585 stands out as the most adverse, with significantly higher costs compared to the other scenarios. Regarding the comparison between adaptation measures, the results indicate clear differences in the economic implications among them.

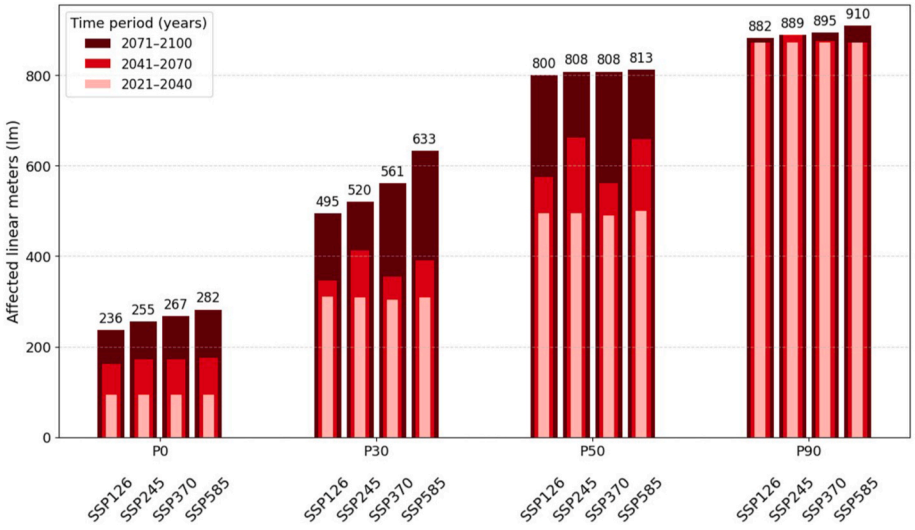

Fig. 12. Visual representation of the affected linear meters for unprotected sections.

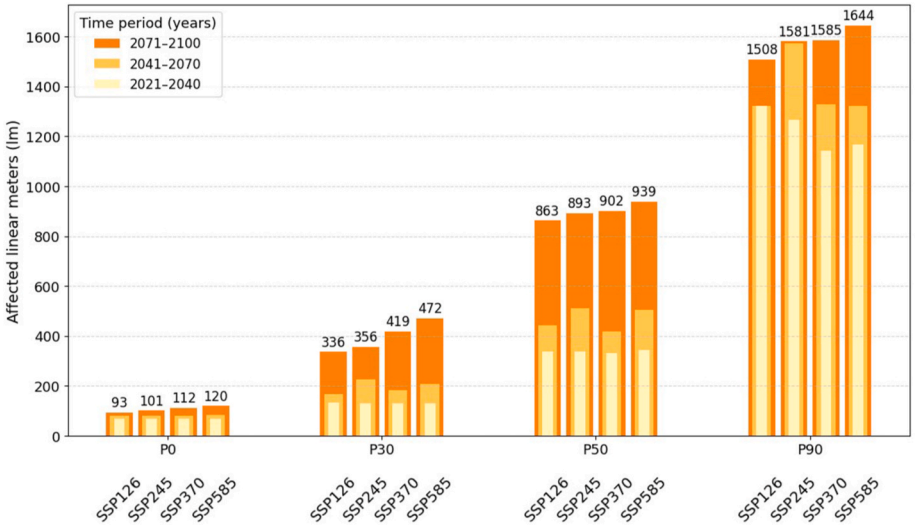

Fig. 13. Visual representation of the affected linear meters for rock revetment-protected sections.

Table 6
Cumulative costs associated with the unprotected sections and adaptation measures comparison.

Climate-scenario	Cumulative time period	Cumulative cost for unprotected sections			Economic comparison Savings		
		BAU	Ad. Measure 1	Ad. Measure 2	AM 1 vs BAU	AM 2 vs BAU	AM 2 vs AM 1
SSP126	2021-2040	53,629,750 €	18,816,500 €	10,556,000 €	64%	80%	45%
	2021-2070	157,284,550 €	50,678,500 €	10,556,000 €	68%	93%	79%
	2021-2100	291,613,550 €	92,463,000 €	21,112,000 €	68%	93%	77%
SSP245	2021-2040	51,809,500 €	18,245,000 €	10,556,000 €	65%	80%	42%
	2021-2070	161,216,200 €	51,728,000 €	10,556,000 €	68%	93%	80%
	2021-2100	292,496,500 €	92,806,000 €	21,112,000 €	68%	93%	77%
SSP370	2021-2040	56,588,550 €	19,740,000 €	10,556,000 €	65%	81%	47%
	2021-2070	158,211,150 €	51,208,000 €	10,556,000 €	68%	93%	79%
	2021-2100	288,361,050 €	92,189,000 €	21,112,000 €	68%	93%	77%
SSP585	2021-2040	62,941,800 €	22,108,000 €	10,556,000 €	65%	83%	52%
	2021-2070	190,985,300 €	61,443,000 €	10,556,000 €	68%	94%	83%
	2021-2100	335,184,200 €	106,962,000 €	21,112,000 €	68%	94%	80%

3.2.1. Unprotected sections

The BAU option consistently leads to the highest cumulative costs, highlighting the financial burden associated with inaction. In the worst-case scenario (SSP585), the implementation and replacement of rock revetment (AM 1) to these sections could result in a 68% of savings in cumulative costs relative to the baseline BAU scenario. Alternatively, the layout modification (AM 2) would yield even greater savings, reaching up to a 94% reduction in cumulative costs. Therefore, comparing both

Table 7
Cumulative costs associated with the rock revetment-protected sections: rock revetment replacement and layout modification comparison.

Climate-scenario	Cumulative time period	Cumulative cost (rock revetment-protected sections)		Economic comparison Savings
		AM A. Rock rev. Replacement	AM B. Layout modification	AM B vs AM A
SSP126	2021-2040	15,719,500 €	19,070,400 €	−18%
	2021-2070	42,595,500 €	19,070,400 €	55%
	2021-2100	85,419,000 €	38,140,800 €	55%
SSP245	2021-2040	15,044,000 €	19,070,400 €	−21%
	2021-2070	44,710,000 €	19,070,400 €	57%
	2021-2100	87,439,500 €	38,140,800 €	56%
SSP370	2021-2040	15,664,000 €	19,070,400 €	−18%
	2021-2070	41,979,000 €	19,070,400 €	55%
	2021-2100	85,227,000 €	38,140,800 €	55%
SSP585	2021-2040	17,652,000 €	19,070,400 €	−7%
	2021-2070	50,498,000 €	19,070,400 €	62%
	2021-2100	99,133,500 €	38,140,800 €	62%

alternatives under the SSP585 climate-scenario, the AM 2 would result in an 80% of savings with respect to the implementation of AM 1.

3.2.2. *Rock revetment-protected sections*

It is evident that rock revetment-protected sections generally incur lower cumulative costs compared to unprotected areas, as they already benefit from some level of structural defence. Accordingly, unlike in unprotected sections, the layout modification measure (AM 2) does not prove to be economically viable during the initial period (2021–2040). Nevertheless, when considering the full-time horizon (2021–2100), AM 2 becomes the most cost-effective option across all climate scenarios. Specifically, under the high-emission scenario SSP585, cumulative costs associated with rock revetment replacement (AM 1) reach 99,133,500 € whereas AM 2 costs remain fixed at 38,140,800 €. This represents a potential cost saving of approximately 62% if AM 2 strategy were adopted instead of repeated rock revetment replacements.

In light of these findings, the cumulative cost of each measure over time is represented for each climate scenario. In this sense, the results for the SSP585 scenario are presented in Fig. 14 and are compared with the outcomes obtained for the remaining scenarios.

In the SSP585 scenario, the economically optimal measure for unprotected sections is clearly identifiable. In this case, the AM 2 becomes more cost-effective than the BAU strategy just four years after the beginning of the analysis. Furthermore, when compared to the implementation of AM 1, AM 2 remains the most economically viable option from year nine onwards. For rock revetment-protected sections, the economic advantage of the AM 2 emerges later, exceeding the cost-effectiveness of rock revetment replacement after 23 years from the start of the analysis.

For the other climate scenarios, the time required for layout modification to become the most favourable alternative is longer. For unprotected sections, layout modification (AM 2) becomes more viable than the BAU approach after six years, and more favourable than rock revetment implementation and replacement (AM 1) after twelve years. In the case of already protected sections, layout modification becomes more cost-effective than rock revetment replacement after 28 years.

4. Discussions

A linear wave propagation model was used to project Hs data near the infrastructure, judged adequate for the study area's characteristics. In line with the development of a model that is both simple and robust, a simplified approach based on linear wave propagation has been preferred over a more complex numerical model accounting for friction. The use of a simplified linear propagation model introduces uncertainty that must be acknowledged when interpreting the results. In shallow coastal environments, linear formulations may overestimate nearshore wave heights because they do not explicitly account for bottom-friction dissipation and other dynamic processes such as nonlinear wave transformation, wave setup, diffraction/reflection by coastal structures, or storm surge–wave interactions. Evidence from a comparable Catalan coastal setting, where linear propagation was benchmarked against SWANOne (UT Delft, 2026), indicated an overestimation of breaking wave height of approximately 14.29% ± 0.36%, suggesting that simplified analytical propagation may yield conservative nearshore wave conditions. If an uncertainty of this order is transferred to the present study, the propagated Hb values would vary by roughly 0.32 - 0.67 m, which would mainly affect cases close to the adopted vulnerability thresholds. Accordingly, the resulting damage and cost estimates should be interpreted as conservative first-order values. In this sense, the proposed framework is more robust for identifying exposed sectors, comparing climate scenarios, and prioritising adaptation pathways than for predicting absolute losses at event scale.

From a coastal management perspective, this simplification is also justified by transferability and operational feasibility. Detailed process-based models require dense bathymetric information, event-scale calibration and higher computational effort, which are not always available to utilities and local coastal managers responsible for screening long linear assets. By contrast, analytical propagation combined with a breaking criterion provides a transparent and reproducible way to estimate the order of magnitude of wave loading and to express its effects probabilistically, which is appropriate for long-term impact assessment and adaptation planning.

The EESL hydrostatic approach was then introduced by incorporating sea level rise (SLR) into the propagated wave height (Hb). This, together with site mapping and PLI classification, allowed for the

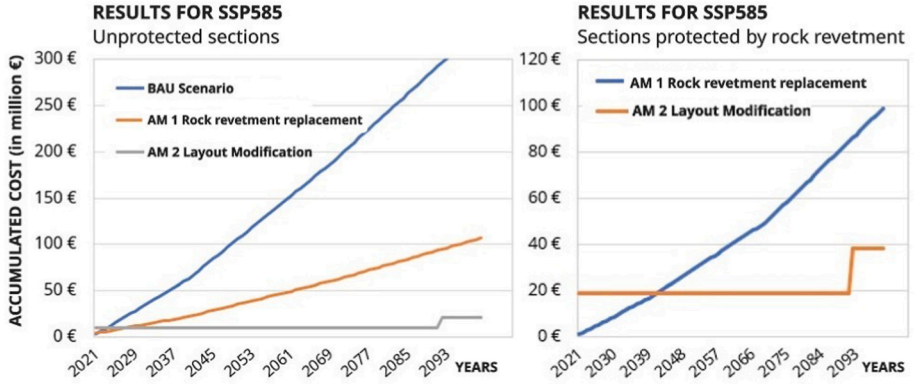

Fig. 14. SSP585 scenario example. Accumulated cost evolution of the adaptation strategies for unprotected sections, (left) and accumulated cost evolution of the adaptation strategies for rock revetment-protected sections (right).

identification of future impacted sections under each climate scenario. The hazard driver (ϕ) enabled relative comparisons between current and projected conditions, supporting the development of vulnerability curves and preliminary cost-risk assessments.

The physical interpretation of Extreme Event Sea Level (EESL) must be considered carefully. Unlike standard ESL metrics reported in the literature, EESL is not intended to represent the exact water level reached during a given event. Instead, it is used as a conservative proxy of coastal loading that combines sea level rise with breaking-wave action in order to identify potentially affected sewer sections. This choice is particularly suited to long-term, scenario-based asset screening, although it may overestimate actual inundation levels when interpreted as a hydrostatic water surface. Consequently, the resulting affected lengths, damage values, and cost estimates should be interpreted as conservative first-order results, more robust for relative comparison among scenarios and adaptation strategies than for precise event-scale reconstruction.

A basic cost–benefit analysis (CBA), considering the BAU scenario and two adaptation options, was also applied to the exposed sections. From a strategic perspective, the comparison of adaptation measures reveals the limitations of reactive approaches such as the ones based on after damage interventions (BAU). In contrast, proactive alternatives, particularly layout modification, demonstrate greater long-term economic efficiency, especially under high-emission scenario (SSP585). While structural defences like rock revetments can temporarily reduce the impacts, their effectiveness diminishes over time, reinforcing the need for more transformative adaptation solutions.

Economic risk estimations suggest substantial potential cost overestimations. Historical expenditures on sewer repairs by Aigües de Barcelona (2017–2023) amounted to €3.8 million, projecting significantly lower future costs (€50–60 million by 2100) compared to the estimated €291 million under scenario SSP126. This discrepancy may be attributed to a combination of factors, including limitations in the vulnerability assessment due to data scarcity, and the use of a hydrostatic modelling approach, which may lead to an overestimation of exposure. The study has been developed using several simplifying assumptions that may contribute to this difference. Firstly, wave direction is not available in the Barcelona buoy dataset; therefore, all storm events have been assumed to originate from the ESE direction, representing the most unfavourable scenario for the Catalan coast. Secondly, the EESL (m) value is assumed to be spatially uniform along the entire length of the sewer for each event. Although this assumption is consistent with the relatively homogeneous coastal conditions in the study area, it may lead to an overestimation of the extent of impact. Nevertheless, the comparison between alternatives is considered valid since historical calibration, future risk estimation, and adaptation measures were all evaluated under the same hazard representation and cost criteria.

The apparent factor-of-four overestimation of cumulative costs is likely explained by the combined effect of several conservative assumptions rather than by the linear propagation model alone. These include the tendency of simplified propagation to overestimate breaking-wave height, the use of a bathtub-based hydrostatic exposure approach, and the uncertainty associated with vulnerability curves derived from limited historical intervention data. In this sense, the methodology should be interpreted as providing conservative first-order estimates of economic impact, while preserving its usefulness for comparing adaptation strategies under a consistent analytical framework.

The vulnerability assessment conducted in this study was designed to be simple yet robust, relying solely on the total costs associated with the repair of the main sewer. It does not include a sensitivity analysis of risk-related factors such as structural, adaptive, or operational resilience, which are also components of the vulnerability. This type of analysis, along with the evaluation of sensitivity in the climatic coastal variables that predominantly influence risk definition, is proposed as future work complementary to the present research. In this regard, a recognised limitation of the methodology is the limited availability of data to develop damage curves linking oceanographic variables with linear damage to the sewer or its protective structures. In this context, the contribution of this research lies in introducing initial order-of-magnitude estimates for the economic valuation of damage. Expanding the database with additional interventions in the sewer, both within the study area and in other comparable sanitation systems, remains a key area for future work aimed at improving the vulnerability assessment.

Comparative analysis underscores similar economic implications across scenarios SSP126, SSP245, and SSP370, while SSP585 emerges as notably adverse, with approximately 13–14% higher costs due to more frequent and intense impacts, more strongly concentrated in the final time period analysed (2071–2100). Among adaptation strategies assessed, layout modification consistently proves most economically viable across both unprotected and rock revetment-protected areas. In unprotected sections, this measure could avoid up to 94% of costs compared to reactive strategies (Business-As-Usual, BAU) and achieve up to 80% cost savings relative to rock revetment implementation in terms of total costs projected up to 2100. In rock revetment-protected sections, layout modifications still offer long-term cost savings of up to 62% relative to rock revetment replacement approach.

A semi-quantitative sensitivity analysis was considered to assess the potential effect of the simplified linear propagation on the economic results. Based on the 14.29% overprediction reported for linear propagation in a comparable Catalan coastal setting, applying an equivalent correction to the Hb values obtained in this study would reduce the wave-related component by approximately 0.32 - 0.67 m, and the associated hazard driver by about 0.06 - 0.12. This effect would mainly influence cases close to the adopted vulnerability thresholds and therefore may lead to an overestimation of absolute damage and cost values, especially for marginal events. However, the same hazard-modelling framework was consistently used for historical damage reconstruction, vulnerability definition, and future scenario assessment. As a result, although the absolute cost estimates should be interpreted with caution, the relative comparison among Business-as-Usual and adaptation alternatives is considered more robust.

5. Conclusions

This study provides a comprehensive assessment of climate-induced risks to coastal wastewater infrastructure, using the Llevant Main Sewer (Badalona) as a case study. By integrating hazard projections, exposure analysis, and vulnerability assessment, the research highlights the relevance and applicability of a structured risk-based framework for evaluating long-term impacts of sea level rise (SLR) and storm surges on coastal sewer systems.

The findings highlight that while significant wave height (Hs) projections exhibit limited sensitivity to different climate scenarios, SLR demonstrates a distinct upward trend across all scenarios, becoming the primary driver of future coastal risk. This observation underscores the importance of focusing adaptation planning around the progressive encroachment of sea level, especially in densely populated coastal areas as the Metropolitan Area of Barcelona. Furthermore, the Cost-Benefit Analysis reveals that, despite its higher upfront investment, sewer relocation consistently outperforms the remaining alternatives across all SSP scenarios in the long term, making it the economically preferred adaptation strategy for the Llevant Main Sewer.

Future applications of this framework could benefit from targeted refinements, particularly improved bathymetric/topographic and shoreline-monitoring data, more systematic georeferenced records of past damage and repair costs, and selective validation of critical sections using more detailed hydrodynamic models. Such improvements would likely refine local calibration and the estimation of absolute losses. However, these data collection and modelling efforts are also costly and time-consuming, both in acquisition and analysis, and their added value

should be assessed against the decision-making needs of coastal managers. In this sense, simplified and transparent approaches remain especially useful for coastal management, because they provide credible order-of-magnitude estimates that support robust screening and adaptation decisions without suggesting a level of precision that future coastal evolution may not justify.

In light of these results, future work could focus on the definition and assessment of additional adaptation measures, particularly in those sections where the sewer can be integrated beneath a seafront promenade. In such contexts, alternative protection strategies aimed at reducing wave impact, such as vertical seawalls with retrofitting solutions, could be explored, as suggested by existing physical modelling studies (Dong et al., 2020). This line of research would contribute to a more robust adaptation framework, aligned with broader international challenges related to sea level rise, which heighten the vulnerability of coastal infrastructure to extreme events.

The transferability of the proposed framework depends on distinguishing between its generic structure and context-specific inputs. While the methodological approach can be applied to other coastal urban systems, its implementation requires local data on hazard conditions, infrastructure characteristics, and cost parameters. Future work should focus on refining these inputs and expanding datasets to enhance the robustness and generalisation of the approach across different geographical contexts.

Despite the inherent uncertainties in hazard modelling and the limitations of data availability in the vulnerability assessment, this structured research offers valuable insights for decision-makers, providing a robust and transferable framework to support climate resilience planning in other urban coastal areas. Prioritising asset-level analysis, as exemplified by the ICARIA project, and integrating it into broader urban resilience strategies will be essential to ensure the long-term functionality of critical infrastructure under evolving climate conditions.

Statements and declarations

Funding

This research has been developed within EU ICARIA project (Improving Climate Resilience of Critical Assets). This project was funded by the European Commission through the Horizon Europe Programme, Grant No. 101093806. https://cordis.europa.eu/project/id/101093806. This research has received financial support from the Industrial Doctorates Programme of the Department of Research and Universities of the Government of Catalonia, under the Grant 2024 DI 00085.

CRediT authorship contribution statement

Guillem Flor Tey: Data curation, Investigation, Methodology, Writing – original draft. **Joan Insa:** Data curation, Formal analysis, Investigation, Methodology. **Eduardo Martínez-Gomariz:** Conceptualization, Supervision, Writing – review & editing. **Beniamino Russo:** Project administration, Resources, Writing – review & editing. **César Mösso:** Writing – review & editing. **César Paradinas:** Data curation, Investigation.

Declaration of competing interest

The authors declare that they have no known competing financial interests or personal relationships that could have appeared to influence the work reported in this paper.

Acknowledgments

The authors would like to thank Aigües de Barcelona, the Metropolitan Company for Integrated Water Cycle Management, for their collaboration through the provision of data and logistical support. The authors thank Oriol Pegueroles, from Aigües de Barcelona, for his collaboration by providing historical interventions data. .

Data availability

Data will be made available on request.

References

AMB, 2024a. Getting to know the metropolitan area. Location and land uses [WWW Document]. Àrea Metroppolitana de Barcelona. URL. https://www.amb.cat/en/web/area-metropolitana/coneixer-l-area-metropolitana.

AMB, 2024b. Medi ambient. Instal·lacions i equipaments [WWW Document]. Àrea Metropolitana de Barcelona. URL. https://www.amb.cat/s/web/medi-ambient/aigua/instalacions-i-equipaments.html.

Bergillos, R.J., 2016. Oleaje y nivel del mar. Dinámica Ambiental. Gestión Integral de Puertos y Costas. Grado de Ingeniería Civil. Especialidad Transportes Y Servicios Urbanos. Granada.

Cahoon, L.B., Hanke, M.H., 2017. Rainfall effects on inflow and infiltration in wastewater treatment systems in a coastal plain region. Water Sci. Technol. 75, 1909–1921. https://doi.org/10.2166/wst.2017.072.

Crichton, D., 1999. The risk triangle. In: Risk Assessment, CGU Insurance. United Kingdom.

Dong, S., Abolfathi, S., Salauddin, M., Tan, Z.H., Pearson, J.M., 2020. Enhancing climate resilience of vertical seawall with retrofitting - a physical modelling study. Appl. Ocean Res. 103. https://doi.org/10.1016/j.apor.2020.102331.

Flood, J.F., Cahoon, L.B., 2011. Risks to coastal wastewater collection systems from sea-level rise and climate change. J. Coast Res. 27, 652–660. https://doi.org/10.2112/JCOASTRES-D-10-00129.1.

Friedrich, E., Kretzinger, D., 2012. Vulnerability of wastewater infrastructure of coastal cities to sea level rise: a South African case study. WaterSA 38, 755–764. https://doi.org/10.4314/wsa.v38i5.15.

Generalitat de Catalunya. Departament d'Acció Climàtica, Alimentació i Agenda Rural. Consell Assessor per al Desenvolupament Sostenible., 2021. Un litoral al límit. Recomanacions per a una gestió integrada de la costa catalana. Informe 1/2021. Barcelona 14–26, 978-84-18986-31-4. https://cads.gencat.cat.

Hu, X., Pant, R., Zorn, C., Lim, W., Koks, E., Mao, Z., 2019. Methodology and Findings for the Exposure Analysis of the Chinese Wastewater Sector to Flooding and Earthquakes Hazards, Methodology and Findings for the Exposure Analysis of the Chinese Wastewater Sector to Flooding and Earthquakes Hazards. World Bank, Washington, DC. https://doi.org/10.1596/1813-9450-8903.

Hughes, J., Cowper-Heays, K., Olesson, E., Bell, R., Stroombergen, A., 2021. Impacts and implications of climate change on wastewater systems: a New Zealand perspective. Clim. Risk Manag. https://doi.org/10.1016/j.crm.2020.100262.

ICGC, 2024. Bessons Digitals - Elevcions. Model d'Elevacions del Terreny de 2x2 m. Institut Cartogràfic i Geològic de Catalunya [WWW Document]. Generalitat de Catalunya. URL. https://www.icgc.cat/ca/Geoinformacio-i-mapes/Dades-i-productes/Bessons-digitals-Elevacions.

IPCC, 2021. Climate Change 2021: the Physical Science Basis. Contribution of Working Group I to the Sixth Assessment Report of the Intergovernmental Panel on Climate Change. https://doi.org/10.1017/9781009157896. Masson-Delmotte, V., Zhai, P., Pirani, A., Connors, S.L., Péan, C., Berger, S., Caud, N., Chen, Y., Goldfarb, L., Gomis, M.I., et al. . New York, NY, USA.

IPCC, 2023. IPCC Sixth Assessment Report. Working Group II. Climate change 2022: impacts, adaptation and vulnerability. Summary for policymakers. In: Climate Change 2022 – Impacts, Adaptation and Vulnerability. Cambridge University Press, pp. 3–34. https://doi.org/10.1017/9781009325844.001.

IPCC, 2023. Summary for policymakers. In: Lee, H., Romero, J. (Eds.), Climate Change 2023: Synthesis Report. Contribution of Working Groups I, II and III to the Sixth Assessment Report of the Intergovernmental Panel on Climate Change [Core Writing Team. https://doi.org/10.59327/IPCC/AR6-9789291691647.001. Geneva, Switzerland.

Kaempfer, W., Berndt, M., 1999. Estimation of Service Life of Concrete Pipes in Sewer Networks. Ottawa.

Kasmalkar, I., Wagenaar, D., Bill-Weilandt, A., Choong, J., Manimaran, S., Lim, N., Rabonza, M., Lallemant, D., 2024. Flow-tub model: a modified bathtub flood model with hydraulic connectivity and path-based attenuation. MethodsX 12, 102524. https://doi.org/10.5281/zenodo.10012208.

Laino, E., Iglesias, G., 2024. Multi-hazard assessment of climate-related hazards for European coastal cities. J. Environ. Manag. 357. https://doi.org/10.1016/j.jenvman.2024.120787.

Leone, M.F., Zuccaro, G., De Gregorio, D., Turchi, A., Tedeschi, A., Büegelmayer-Blaschek, M., Sfetsos, A., Zarikos, I., Coronas, A. de la C., Russo, B., 2025. A holistic asset-level modelling framework for a comprehensive multi-hazard risk/impact assessment: insights from the ICARIA project. Int. J. Disaster Risk Reduct. 119. https://doi.org/10.1016/j.ijdrr.2025.105319.

Martínez-Gomariz, E., Forero-Ortiz, E., Guerrero-Hidalga, M., Castán, S., Gómez, M., 2020. Flood depth-damage curves for Spanish urban areas. Sustainability 12. https://doi.org/10.3390/su12072666.

Martínez-Gomariz, E., Guerrero-Hidalga, M., Forero-Ortiz, E., Gonzalez, S., 2021. Citizens' perception of combined sewer overflow spills into bathing coastal areas. Water Air Soil Pollut. 232. https://doi.org/10.1007/s11270-021-05305-x.

Megías, E., García-Román, M., 2024. Naturaleza dispersiva de los swells que llegan a Canarias desde el Atlántico Sur. Estudio del caso paradigmático de los eventos registrados durante el verano de 2023. Ingeniería del Agua 28, 297–309. https://doi.org/10.4995/ia.2024.22425.

Meta Engineering, 2021. Estudi d'alternatives de traçat de col·lector de Llevant als termes municipals de Badalona i Sant Adrià del Besòs. Tram 1. AB/RIM/2019/48). Barcelona.

NOAA, 2024. Is Sea Level Rising? Yes, Sea Level is Rising at an Increasing Rate. National Ocean Service. National Oceanic and Atmospheric Administration [WWW Document]. URL. https://oceanservice.noaa.gov/facts/sealevel.html. accessed 5.21.25.

Paradinas, C., Prado, C., Galiano, L., Redolat, D., Monjo, R., Gaitan, E., 2024. ICARIA: spatially distributed climate projections from statistical downscaling. Zenodo. https://doi.org/10.5281/zenodo.12930101 [Data set].

Puertos del Estado, 2004. Extremos Máximos De Oleaje Por Direcciones. Boya de Barcelona.

ROM, 1992. Recomendaciones Para Obras Marítimas ROM 0.3-91 OLEAJE Anejo I. Clima Marítimo En El Litoral Español. Ministerio De Obras Públicas Y Transportes. Dirección General de Puertos.

Russo, B., de la Cruz Coronas, À., Leone, M., Evans, B., Brito, R.S., Havlik, D., Bügelmayer-Blaschek, M., Pacheco, D., Sfetsos, A., 2023. Improving climate resilience of critical assets: the ICARIA Project. Sustainability 15. https://doi.org/10.3390/su151914090.

Russo, B., Velasco, M., Locatelli, L., Sunyer, D., Yubero, D., Monjo, R., Martínez-Gomariz, E., Forero-Ortiz, E., Sánchez-Muñoz, D., Evans, B., Gonzalez Gómez, A., 2020. Assessment of Urban Flood Resilience in Barcelona for Current and Future Scenarios. The RESCCUE Project. From Climate and Hydrological Hazards to Risk Analysis and Measures. Sustainability 12, 5638. https://doi.org/10.3390/su12145638.

Sangsefidi, Y., Bagheri, K., Davani, H., Merrifield, M., 2023. Data analysis and integrated modeling of compound flooding impacts on coastal drainage infrastructure under a changing climate. J. Hydrol. (Amst). 616. https://doi.org/10.1016/j.jhydrol.2022.128823.

SMC, 2021. Estudio De La Evolución De Los Temporales De Mar Históricos En La Costa Catalana a Partir De Las Observaciones Y Las Simulaciones Marítimas (1990-2020). Barcelona.

Spirandelli, D., Babcock, R., Shen, S., 2018. Assessing the Vulnerability of Coastal Wastewater Infrastructure to Climate Change. University of Hawai'i Sea Grant College Program.

Tebaldi, C., Strauss, B.H., Zervas, C.E., 2012. Modelling sea level rise impacts on storm surges along US coasts. Environ. Res. Lett. 7. https://doi.org/10.1088/1748-9326/7/1/014032.

UPC, 2014. Oleaje. Propagación. Enginyeria De Costes. Enginyeria Civil. Universitat Politècnica de Catalunya, Barcelona.

UT Delft, 2026. SWAN scientific and technical documentation. SWAN Cycle III Version 41.51. Delft University of Technology, Delft, The Netherlands. http://www.swan.tudelft.nl.